Positive binding energy of a biexciton confined in a localization center formed in a single $In_xGa_{1-x}N/GaN$ quantum disk

R. Bardoux,[1] A. Kaneta,[1,3] M. Funato,[1,3] Y. Kawakami,[1,3] A. Kikuchi,[2,3] and K. Kishino[2,3]
[1]*Department of Electronic Science and Engineering, Kyoto University, Kyoto 615-8510, Japan*
[2]*Department of Electronical and Electronics Engineering, Sophia University, Tokyo 102-8554, Japan*
[3]*CREST, Japan Science and Technology Agency, Kawaguchi, Saitama 330-0012, Japan*
(Received 24 December 2008; revised manuscript received 26 January 2009; published 8 April 2009)

We report microphotoluminescence spectroscopy performed on individual and ensemble InGaN/GaN quantum disks (Q-disks). The typical spectrum of a single Q-disk exhibited the contribution of localization centers (LCs) formed in the InGaN active layer of the Q-disks, characterized by sharp lines appearing on the low energy side of the spectra. In addition, a broader emission peak identified as the luminescence of the quasi-two-dimensional (2D) InGaN active layer surrounding the LCs appears systematically at higher energy. Time-resolved photoluminescence experiment performed on single Q-disks exhibited the excitonic transfer, from the 2D InGaN active layer to LCs, at the submicroscopic scale. Excitation power dependence studies and linear polarization analysis allowed us to identify a biexciton complex confined in a LC in a single Q-disk with a surprising positive binding energy of 13 meV. The absence of screening effect by increasing the excitation power density and the fast excitonic radiative lifetime of a few hundred picoseconds that we measured on several individual Q-disks indicate that the absence of internal electric field in the structure can explain the observed positive biexciton binding energy.

DOI: 10.1103/PhysRevB.79.155307 PACS number(s): 73.21.Hb, 72.15.Rn, 73.21.La, 73.22.Dj

I. INTRODUCTION

In the last decades, III-nitride-based semiconductors have attracted increasing interest for achievement of light-emitting devices in ultraviolet (UV) spectral range and for their original physical properties such as the quantum confined Stark effect (QCSE) induced by the presence of an internal electric field in the hexagonal crystallographic phase. Indeed, the wurtzite symmetry allows for the presence of both spontaneous and piezoelectric polarizations that have particularly large magnitudes in GaN, AlN, InN, or their alloys.[1] In the case of low-dimensional objects such as quantum dots (QDs), the difference of total polarization between the smaller and the larger band-gap materials induces extremely large electric fields along the (0001) growth axis, which have the disadvantage to decrease drastically the internal quantum efficiency (η_{int}) of the heterostructure.

Among the III-nitride-based compounds, those based on InGaN material are one of the most promising for the achievement of light-emitting diodes (LEDs) in the visible spectral range. Indeed, light-emitting devices embedding InGaN/GaN quantum heterostructures give the opportunity to control the emission wavelength from near infrared to UV just by changing the indium mole ratio in the $In_xGa_{(1-x)}N$ active layer.[2] Moreover, it is well known that in ternary alloys,[3] localization centers (LCs) induced by local fluctuations of the In mole fraction at a few nanometer scales exhibit a strong contribution to the radiative recombination processes of the active layer;[4,5] these LCs, by hindering nonradiative recombination processes, confer to these heterostructures' higher η_{int} compared to other binary III-nitride-based materials.

The one-dimensional nanocrystals called nanocolumns constitute an important issue in the application field of III-nitride-based heterostructures.[6,7] Indeed, these nanocolumnar heterostructures that we call quantum disks (Q-disks) exhibit better crystallographic properties compared to conventional quantum wells (QWs) and lead to a sizeable improvement of the η_{int}.[8,9] Recently, Kikuchi *et al.*[10] fabricated InGaN/GaN nanocolumnar LEDs in which green to red light emissions have been achieved under direct current operation at room temperature.

Despite these encouraging advances, the knowledge on the physical properties of the Q-disks is very limited; until today just a few optical studies on individual Q-disks[11] have been reported. However, these kinds of investigations are quite required for an inmost understanding of their optical properties. Besides, as a Q-disk has a diameter of about a few tens of nanometer, these nanostructures are laterally limited by their side wall. Consequently, the strain relaxation of their layers has a particular and complex aspect compared to the one of a conventional QW (Ref. 8) and will obviously lead to original optical properties that still have to be clarified. While the existence of the internal electric field and the presence of LCs have been well studied in the case of conventional QWs, their existence and their role in the radiative recombination processes have not been investigated yet at the scale of a single Q-disk. However, the spectroscopic studies of individual Q-disk are indispensable for a deep comprehension of their basic physical properties.

In this paper, we report microphotoluminescence (μPL) studies performed on individual and ensemble of nanocolumnar heterostructures constituted by a single InGaN/GaN QW. We exhibited the contribution of localized center in the radiative recombination processes of single InGaN/GaN Q-disk. We analyzed deeply the optical properties of several quantum disks by power dependence, linear polarization, and time-resolved photoluminescence (TRPL). By TRPL measurements, we exhibited excitonic transfer effect from the two-dimensional (2D) InGaN layer to LCs at the scale of a

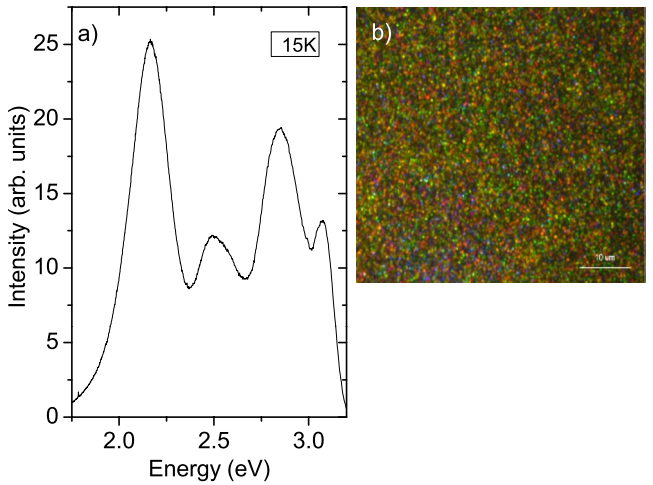

FIG. 1. (Color online) (a) Macroscopic PL spectrum. (b) a μPL image performed on an ensemble of Q-disk.

single Q-disk. We could identify a biexciton complex confined in a LC formed in a single Q-disk. The optical characteristics of this biexciton compared with other results obtained on single and ensemble of Q-disks lead us to the conclusion that the internal electric field is drastically reduced in the Q-disk structure.

II. EXPERIMENTAL RESULTS

The self-organized Q-disks were grown by molecular-beam epitaxy (MBE) with a nitrogen-plasma source on (0001)-oriented sapphire substrates. The Q-disks are composed of a 1.45 μm GaN buffer layer, a 5 nm InGaN active layer, and a 35 nm GaN capping layer. According to scanning electron microscopy (SEM) images, the lateral size of the Q-disks ranged between 80 and 150 nm. In Fig. 1(a), we plotted the spectrum of an ensemble of Q-disks (about 10 000 Q-disks are excited) under an excitation power density of about 4 kW/cm^2. Four emission peaks are observed centered at 2.15, 2.48, 2.84, and 3.07 eV. The optical microscope images [see Fig. 1(b)] of this sample exhibited that from a Q-disk to another, different emission wavelengths from blue to red are observed. Thus, we attributed each one of these emission peaks to a Q-disk family characterized by a specific In ratio in the InGaN active layer.

To isolate the photoluminescence (PL) signal emitted by an individual Q-disk, the deposited nanocolumns had been removed by a mechanical scriber technique and dispersed in a pure water solution. By drying a drop of this solution on a Si substrate covered by aluminum, we obtained a diluted nanocolumn samples with a superficial density of about 2.5 $\times 10^8$/cm^2 such that we were able to isolate spatially the signal emitted by a single Q-disk. Excitation and collection of the luminescence were performed perpendicular to their growth direction through a 40$\times$ optical objective lens. The laser spot had a diameter of 1 μm. The sample was cooled in a continuous flow helium cryostat at 8 K (if not specified). The Q-disks were excited below the GaN band gap, with a frequency doubled Ti-Sapphire at 375 nm. The luminescence

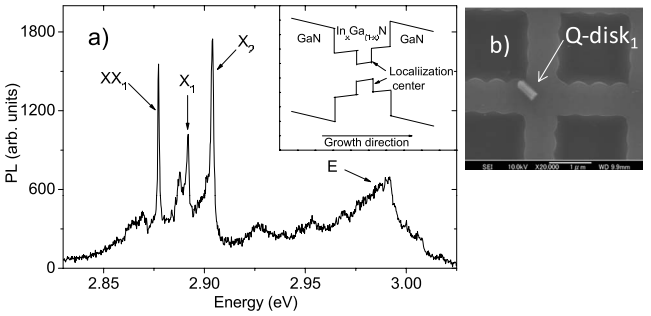

FIG. 2. (a) μPL spectrum of a single Q-disk (called Q-disk$_1$) at 20 K. Inset image: schematic illustration of a Q-disk band structure according to our experimental results. (b) Scanning electron microscopy image of the Q-disk$_1$.

was dispersed by a 60 cm spectrometer with a 1200 groves/mm grating coupled to a nitrogen-cooled charged-couple device (CCD), with a spectral resolution of 1 meV. In TRPL experiments, the luminescence was analyzed using a Streak camera with a time resolution of 10 ps.

Figure 2(a) shows the spectrum of a single InGaN/GaN Q-disk (called Q-disk$_1$) obtained at 20 K, under an excitation power density of 5 kW/cm^2; a SEM image of this quantum disk is shown in Fig. 2(b). On the low energy side of the spectrum, sharp emission lines appeared (X_1, XX_1, and X_2) with a full width at half maximum (FWHM) of 1 meV (limited by our spectral resolution); at higher energy, a broader emission peak (E) is observed with a FWHM of 25 meV. These two types of emission peaks appeared systematically in the spectra of about 20 Q-disks, with the same energy hierarchy. As previously reported in conventional InGaN/GaN QWs,[4] these sharp lines reveal the existence of LCs in the InGaN active layer of the Q-disks. By increasing the excitation power density from 100 W/cm^2 to 10 kW/cm^2 the FWHM of the broad peak E is enhanced from 10 to 60 meV. This broader peak must be related to the confinement potential induced by the 2D InGaN layer embedded between the GaN barriers. The non-Gaussian and asymmetric aspect of this peak reveals the existence of thickness and/or In ratio fluctuations on a larger spatial scale than the LCs.

The spectrum of the Q-disk$_1$ can be considered as a typical one; that is to say, the sharp emission lines appearing in addition of a broader peak at higher energy have been observed systematically in the spectra of the investigated Q-disks. In accordance with our experimental results obtained on about twenty Q-disks, in the inset image from Fig. 2(a), a schematic description illustrating the band structure aspect of the Q-disks is presented. As the LCs are emitting at lower energy than the 2D InGaN/GaN Q-disk, we concluded that the LCs are caused by a local enhancement of the In mole fraction or of the InGaN thickness.

A. Biexciton complex

We studied the excitation power dependence of the Q-disk$_1$'s spectrum under an excitation power density that ranged from 120 W/cm^2 to 500 kW/cm^2. In Fig. 3, we plotted the integrated intensity of the emission lines X_1, XX_1,

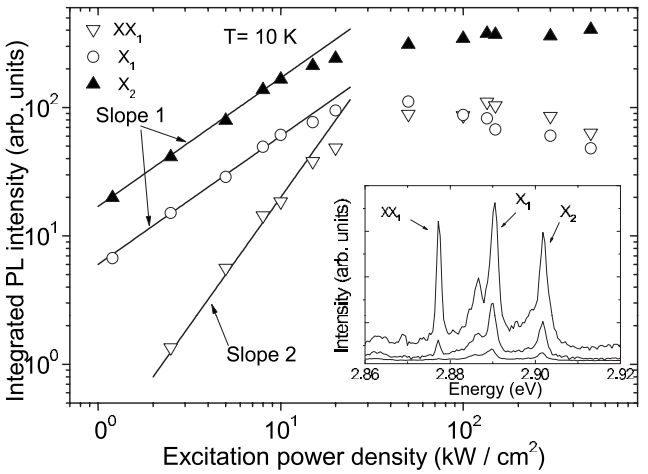

FIG. 3. Integrated intensity of the emission lines X_1, XX_1, and X_2 as a function of the excitation power density plotted in bilogarithmic scale. The solid lines show the linear power-law fitting results. Inset image: spectra of the Q-disk$_1$ under three different excitation power densities: 120, 220, and 2.5×10^3 W/cm^2.

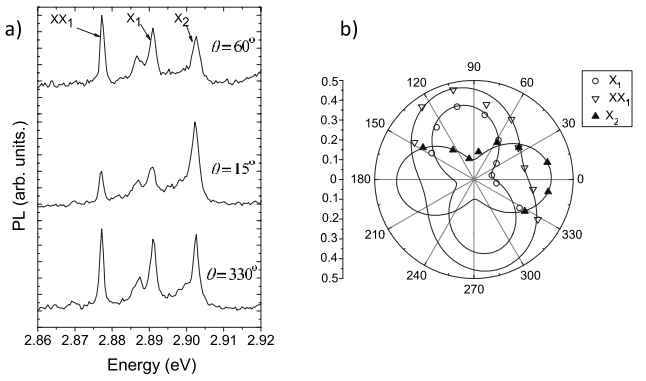

FIG. 4. (a) μPL spectra of the Q-disk$_1$ analyzed at three different angles θ. (b) Polar representation of the integrated intensity of the emission lines X_1, XX_1, and X_2 as a function of the analyzer angle over 180°. The angle θ=0° is *a priori* not related to any crystallographic direction of the Q-disk structure.

and X_2 as a function of the excitation power density. As showed in the inset of Fig. 3 the peak XX_1 was observed only from an excitation power density of about 220 W/cm^2. Below the saturation regime observed above 20 kW/cm^2, while the intensity of X_1 and X_2 varies linearly, the quadratic dependency of XX_1 reveals the existence of a biexciton complex in a LC of the Q-disk$_1$.

To determine the binding energy of the biexciton XX_1 we have to determine the excitonic state related to XX_1. For this purpose, we investigated the exciton fine structure of the LCs.

B. Fine structure: biexciton binding energy

Figure 4(a) shows the spectra of the Q-disk$_1$ acquired at three different analyzer angles (θ). In Fig. 4(b) we plotted the integrated intensity $[I(\theta)]$ of X_1, X_2, and XX_1 for θ varying over 180°. The angular dependency of their integrated intensity exhibited a linear polarization, well described by the following relation: $I(\theta)=a+b\cos^2(\theta-\theta_0)$, where a and b are two adjustable constants and θ_0 is the polarization angle of the emission line (i.e., $I(\theta_0)$ is the maximum value). This effect has been well reported in the case of cubic phase QDs[12,13] and is called exciton fine structure. This optical property is the signature of the valence-band mixing induced by the in-plane anisotropy of strain and/or QD or QD-like shape. In the case of the cubic phase QDs, the excitonic fine structure is optically characterized by two cross linearly polarized states Π_x and Π_y (parallel to the crystallographic axis) with the same integrated intensity and split by a few meV via the *e-h* spin exchange interaction. In the case of hexagonal crystallographic heterostructure, as reported in Ref. 14 and as observed in our results (see Fig. 4), the exciton fine structure characteristics is strongly different with those obtained with the cubic phase QDs. Indeed, as we can see in Fig. 4, the emission lines are not fully polarized ($a\neq0$); their polarization angle θ_0 is not correlated with any crystallographic axis (the polarization angles of X_1 and X_2 are separated by 104°); and within our spectral resolution of 1 meV, no cross polarized doublets are observed. Generally speaking, we observed the same linear polarization effect on 90% of the Q-disks that we investigated. As the fine structure involves symmetry breakage at the scale of the exciton Bohr radius, this results confirm the zero-dimensional (0D) character of the excitonic confinement potential of the LCs.

Moreover, the radiative recombination of a given biexciton state XX will leave an exciton X in an intermediate state according to the following relation: $XX\rightarrow X+h\nu_{XX}$, where $h\nu_{XX}$ represent the photon energy emitted by this process. As pointed out by Kulakovskii *et al.*[15] in the case of CdSe QDs, since the biexciton ground state is a spin-singlet state, the polarization of the biexciton states is determined by the intermediate excitonic state X. In other words, if the emission line of the biexciton is linearly polarized, its polarization angle must be the same as the associated excitonic emission line. As shown in Fig. 4(b), the biexciton emission line XX_1 and the exciton emission line X_1 have the same polarization angle. Thus, we can conclude unambiguously that the biexciton state XX_1 and the exciton state X_1 are associated and emitted by the same LC. Then, we determined a positive biexciton binding energy E^b_{XX} of 13 meV; later in this paper further discussions will be held on this value.

C. Time-resolved photoluminescence

In Fig. 5, we plotted the PL intensity decay of an ensemble of Q-disks. A biexponential function has been chosen to fit the experimental data. Two recombination regimes are observed. To know if these two regimes are due to a collective effect or related to the intimate recombination process of a given Q-disk we performed TRPL on individual Q-disks. The TRPL experiment has been performed on the Q-disk$_1$ under an excitation density of 1 kW/cm^2, below the saturation regime of the biexciton complex observed in Fig. 3. The experimental data are plotted in Fig. 6 for the three excitonic states i ($i=X_1;XX_1;E$). As the intensity decay $[I^i(t)]$ of these three excitonic states exhibited two recombination regimes, a

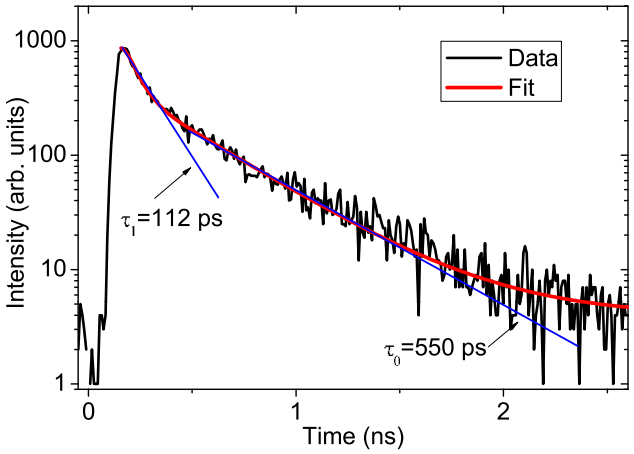

FIG. 5. (Color online) Time dependence of the PL intensity of an ensemble of Q-disks emitting around 2.9 eV [see Fig. 1(a)]; the vertical axis is in logarithmic scale. The data had been fitted by a biexponential function.

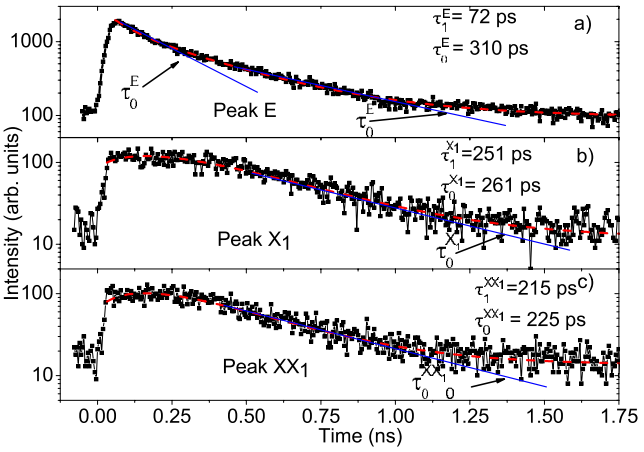

FIG. 6. (Color online) Time dependence of the μPL intensity of (a) the emission peak E, and the emission lines (b) X_1 and (c) XX_1. The dashed line is the biexponential fit obtained for each decay curve. The vertical axis is in logarithmic scale.

biexponential function has been chosen for the fitting, such as

$$I^i(t) = A_1^i \exp\left(-\frac{t}{\tau_1^i}\right) + A_0^i \exp\left(-\frac{t}{\tau_0^i}\right), \quad (1)$$

where A_1^i and A_0^i are two constants and τ_1^i and τ_0^i are the characteristic time of the two successive decay regimes of the excitonic state i; τ_0^i correspond to the radiative lifetime of the excitonic states i extrapolated in the second decay regime.

The characteristic recombination time of the first regime of the emission peak E is given by τ_1^E=72 ps. This regime can *a priori* be attributed to three different effects: the QCSE, as for other III-nitride heterostructures;[16] the exciton/carrier transfer from the InGaN layer to the lower energy states such as localization center states;[4,17] and the nonradiative recombination processes.[18] As it will be discussed later in this paper, we assumed that the effect of an eventual internal electric field is negligible; thus one can write the following relation:[18]

$$\frac{1}{\tau_1^E} = \frac{1}{\tau_{tr}} + \frac{1}{\tau_{Nrad}}, \quad (2)$$

where $\frac{1}{\tau_{tr}}$ is the exciton transfer rate from the InGaN layer to lower energy level and $\frac{1}{\tau_{Nrad}}$ is the nonradiative recombination rate. The exciton transfer from the InGaN layer to localization centers is well illustrated by the dynamic of the emission lines X_1 and XX_1 [shown in Figs. 6(b) and 6(c), respectively]: during the first 300 ps after the laser pulse (at t=0), the intensity of X_1 and XX_1 remains almost constant so that to fit the first decay regime of the emission lines X_1 and XX_1, we chose $A_1^i < 0$ [see Eq. (1)]. This behavior demonstrates a continuous feeding of the localization center by e-h pairs originally photocreated in the InGaN layer. The rate of e-h pairs transferred from the InGaN layer controls the radiative recombination dynamic of the LCs. The exciton transfer time τ_1^i from the InGaN layer to the localization states X_1 and XX_1 is about 251 and 215 ps, respectively (see Fig. 6). By considering an average exciton transfer time from the InGaN layer to the localization center of about 233 ps and the expression of τ_1^E given above, we determined a nonradiative lifetime τ_{Nrad} of about 100 ps in the InGaN layer and deduced an internal quantum efficiency of 24% at room temperature, which is more than two times better than the value reported for conventional InGaN/GaN QWs.[19]

Another interesting feature is that the ratio $\tau_0^{X_1}/\tau_0^{XX_1}$ ($\simeq$1) is different to the commonly accepted value of 2. Indeed, as a photon can only have two different spin states, $|+1\rangle$ or $|-1\rangle$, on the four quantum states available for an exciton confined in a 0D system, only two of these states (called bright states) conduct to a radiative recombination, while the two other states (called dark states) are not radiatively active. If there is no symmetry breakage in the 0D confinement potential, the bright and dark states are degenerated and the probability of finding an exciton in one of these four states after the recombination of the biexciton state is equal to 1/4. Hence, the probability for an exciton to be in a bright state is 1/2 and leads to a radiative lifetime two times larger for the exciton than for the biexciton. However, when a symmetry breakage appears in the in-plane confinement potential, the fourfold degenerated excitonic state is lifted via the Coulomb exchange interaction. Consequently, as pointed out by Bacher *et al.*,[20] the spin-flip time between the bright and dark states becomes longer than the radiative lifetime of the exciton, which leads to a ratio of $\tau_0^{X_1}/\tau_0^{XX_1} \simeq 1$. The existence of the exciton fine structure that we discussed above underlies this idea and explains why the exciton state and the biexciton state have the same radiative lifetime.

D. Discussion

The radiative lifetime of about 300 ps that we measured for all the excitonic states of the InGaN Q-disk$_1$ is compatible with our results presented in Fig. 5, obtained on an ensemble of Q-disks, where a radiative lifetime of about 550 ps has been measured. Nevertheless, these measured radiative lifetimes are more compatible with those usually reported

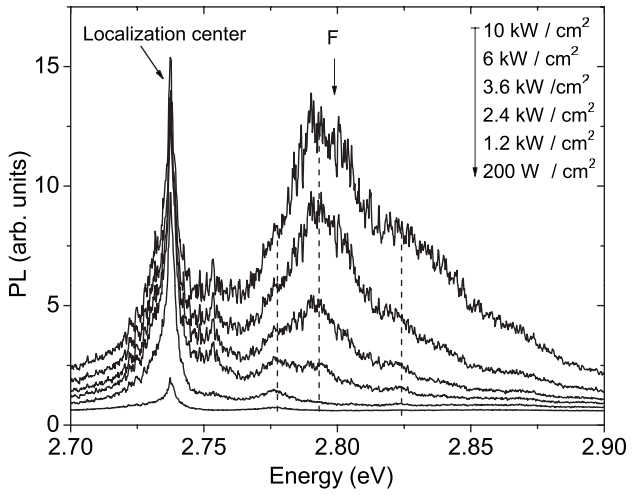

FIG. 7. Excitation power density dependence of the μPL spectra of a single InGaN/GaN Q-disk (called Q-disk$_2$) acquired at 10 K.

from heterostructures without internal electric field such as *II-VI* compounds[21] and nonpolar III-nitride-based compounds[22,23] than those reported for conventional InGaN QWs[23,24] or other III-nitride-based compounds in hexagonal crystallographic phase. Indeed, in hexagonal phase heterostructures, the presence of an internal electric field decreases the oscillator strength of the *e-h* pairs[3,16] and then increases their radiative lifetime. The latter effect is caused by the on-axis separation of electron and hole wave functions by the electric field. Moreover, due to the QCSE, a screening effect of the internal electric field is expected, induced by the photoinjected *e-h* pairs.[16] This effect is optically characterized by a blueshift in the emission peak of the active layer by increasing the *e-h* pairs density. During our study, we never observed such a blueshift in the spectra of the individual Q-disks, as illustrated in Fig. 7 where the excitation power dependence of the μPL spectrum of a single InGaN/GaN Q-disk (called Q-disk$_2$) is plotted. In Fig. 4, a sharp line (signature of the luminescence of a localization center) is observed on the low energy side, in addition of a broader peak (called *F*) at higher energy emitted by the quasi-2D InGaN/GaN confinement potential of the Q-disk$_2$. The important point that we wish to outline here is that no blueshift occurred in the peak emission *F* by increasing the excitation power density. We made the same measurement for more than 20 individual Q-disks, but we never observed any blueshift in the peak originated from the 2D confinement potential of the Q-disks heterostructure. Nevertheless, this blueshift has been observed in conventional InGaN QWs structure as reported in Ref. 23 and consequently expected in our nanocolumnar heterostructure because of the large thickness of the InGaN layer (5 nm) (see Fig. 7).

The absence of screening effect and the short exciton radiative lifetime in the Q-disks constitute a strong indication that the internal electric field is vanished and can explain the observed positive biexciton binding energy never reported until today in InGaN QW and Q-disks. Indeed, in an electric-field-free environment, the sum of all the Coulomb interaction terms between the four fermion particles constituting a biexciton complex is dominated by the attractive terms between the opposite charges. Consequently, E_{XX}^b remains positive in bulk materials. Conversely, in the presence of an internal electric field, the opposite charges (the electrons on one side and the holes on another side) are separated along the growth direction of the heterostructure due to the QCSE. Thus, the sum of the repulsive Coulomb interaction terms between the electrons on one side and the holes on another side will be predominant.[25] It is the reason why, in conventional InGaN QWs, the biexciton binding energy measured in localization centers is negative, with typical E_{XX}^b amplitude of 5 meV.[4] The particular strain distribution in the Q-disks,[8] directly related to the existence of their side wall surface, is probably the origin of a drastic modification of the piezoelectric field in the InGaN and GaN layers. Thus, such an original piezoelectric field induced by the morphology of the Q-disks may explain why any effect of an internal electric field does not appear in our results. Inmost understanding of this aspect will ask an accurate modeling of the strain distribution state of the Q-disks crystallographic structure.

III. CONCLUSION

We identified LCs with 0D confinement potential in the InGaN active layer of the Q-disks. We exhibited at the submicroscopic scale the carrier transfer from the 2D InGaN layer to LCs. Contrary to earlier reports on the negative binding energy in *c*-oriented nitride QDs we measured a positive biexciton binding energy of 13 meV in a LC. The sign of this biexciton binding energy is compatible with all our results obtained on single and ensemble of Q-disks, which indicate that the internal electric field is vanished in these nanocolumnar heterostructure. If these results call for a careful calculation of the strain distribution in the layers of the nanocolumnar heterostructure in conjunction with precise structure analysis, they reveal one more interest of the InGaN/GaN Q-disks in a field where the reduction in the QCSE of the III-nitride-based heterostructures constitutes a stimulating and challenging topic.[25]

ACKNOWLEDGMENTS

Part of this study was supported by a Grant-in-Aid for Scientific Research from the Japan Society for the Promotion of Science and the Global Center of Excellence (G-COE) program, originated from the Ministry of Education, Culture, Sports and Technology (MEXT). Also, we would like to acknowledge Koichi Okamoto for his constructive remarks.

[1] F. Bernardini, V. Fiorentini, and D. Vanderbilt, Phys. Rev. B **56**, R10024 (1997).
[2] W. Shan, W. Walukiewicz, E. E. Haller, B. D. Little, J. J. Song, M. D. McCluskey, N. M. Johnson, Z. C. Feng, M. Schurman, and R. A. Stall, J. Appl. Phys. **84**, 4452 (1998).
[3] P. Lefebvre, J. Allègre, B. Gil, A. Kavokine, H. Mathieu, W. Kim, A. Salvador, A. Botchkarev, and H. Morkoç, Phys. Rev. B **57**, R9447 (1998).
[4] H. Schömig, S. Halm, A. Forchel, G. Bacher, J. Off, and F. Scholz, Phys. Rev. Lett. **92**, 106802 (2004).
[5] K. P. O'Donnell, R. W. Martin, and P. G. Middleton, Phys. Rev. Lett. **82**, 237 (1999).
[6] M. Yoshizawa, A. Kikuchi, M. Mori, N. Fujita, and K. Kishino, Jpn. J. Appl. Phys., Part 2 **36**, L459 (1997).
[7] M. Yoshizawa, A. Kikuchi, N. Fujita, K. Kushi, H. Sasamoto, and K. Kishino, J. Cryst. Growth **189-190**, 138 (1998).
[8] J. Ristic, E. Calleja, A. Trampert, S. Fernandez-Garrido, C. Rivera, U. Jahn, and K. H. Ploog, Phys. Rev. Lett. **94**, 146102 (2005).
[9] K. Kishino, A. Kikuchi, H. Sekiguchi, and S. Ishizawa, Proc. SPIE **6473**, 64730T (2007).
[10] A. Kikuchi, M. Kawai, M. Tada, and K. Kishino, Jpn. J. Appl. Phys., Part 2 **43**, L1524 (2004).
[11] Y. Kawakami, S. Suzuki, A. Kaneta, M. Funato, A. Kikuchi, and K. Kishino, Appl. Phys. Lett. **89**, 163124 (2006).
[12] M. Sugisaki, H.-W. Ren, S. V. Nair, K. Nishi, S. Sugou, T. Okuno, and Y. Masumoto, Phys. Rev. B **59**, R5300 (1999).
[13] M. Bayer, G. Ortner, O. Stern, A. Kuther, A. A. Gorbunov, A. Forchel, P. Hawrylak, S. Fafard, K. Hinzer, T. L. Reinecke, S. N. Walck, J. P. Reithmaier, F. Klopf, and F. Schäfer, Phys. Rev. B **65**, 195315 (2002).
[14] R. Bardoux, T. Guillet, B. Gil, P. Lefebvre, T. Bretagnon, T. Taliercio, S. Rousset, and F. Semond, Phys. Rev. B **77**, 235315 (2008).
[15] V. D. Kulakovskii, G. Bacher, R. Weigand, T. Kümmell, A. Forchel, E. Borovitskaya, K. Leonardi, and D. Hommel, Phys. Rev. Lett. **82**, 1780 (1999).
[16] T. Bretagnon, P. Lefebvre, P. Valvin, R. Bardoux, T. Guillet, T. Taliercio, B. Gil, N. Grandjean, F. Semond, B. Damilano, A. Dussaigne, and J. Massies, Phys. Rev. B **73**, 113304 (2006).
[17] L. Besombes, L. Marsal, K. Kheng, T. Charvolin, L. S. Dang, A. Wasiela, and H. Mariette, J. Cryst. Growth **214-215**, 742 (2000).
[18] A. Kaneta, T. Mutoh, G. Marutsuki, Y. Narukawa, T. Mukai, Y. Kawakami, and Sg. Fujita, Appl. Phys. Lett. **83**, 3462 (2003).
[19] Y. Narukawa, Y. Kawakami, S. Fujita, and S. Nakamura, Phys. Rev. B **59**, 10283 (1999).
[20] G. Bacher, R. Weigand, J. Seufert, V. D. Kulakovskii, N. A. Gippius, A. Forchel, K. Leonardi, and D. Hommel, Phys. Rev. Lett. **83**, 4417 (1999).
[21] M. Colocci, M. Gurioli, and J. Martinez-Pastor, J. Phys. IV **3**, 3 (1993).
[22] F. Rol, S. Founta, H. Mariette, B. Daudin, L. S. Dang, J. Bleuse, D. Peyrade, J. M. Gérard, and B. Gayral, Phys. Rev. B **75**, 125306 (2007).
[23] M. Funato and Y. Kawakami, J. Appl. Phys. **103**, 093501 (2008).
[24] X. H. Zhang, W. Liu, and S. J. Chua, J. Cryst. Growth **268**, 521 (2004).
[25] P. Waltereit, O. Brandt, A. Trampert, H. T. Grahn, J. Menniger, M. Ramsteiner, M. Reiche, and K. H. Ploog, Nature (London) **406**, 865 (2000).